25. Rozsnyai, L. F. and Wrighton, M. S., Selective deposition of conducting polymers via monolayer photopatterning. *Langmuir*, 1995, **11**, 3913–3920.
26. Gorman, C. B., Biebuyck, H. A. and Whitesides, G. M., Fabrication of patterned electrically conducting polypyrrole using self-assembled monolayer: A route to all organic circuits. *Chem. Mater*., 1995, **7**, 526–529.
27. Huang, Z., Wang, P.-C., Macdiarmid, A. G., Xia, Y. and Whitesides, G. M., Selective deposition of conducting polymers on hydroxyl terminated surfaces with printed monolayers of alkylsiloxanes as templates. *Langmuir*, 1997, **13**, 6480–6484.
28. Nishizawa, M., Miwa, Y., Matsue, T. and Uchida, I., Surface pretreatment for electrochemical fabrication of ultrathin patterned conducting polymers. *J. Electrochem. Soc*., 1993, **140**, 1650–1655; Nishizawa, M., Shibuya, M., Sawaguchi, T., Matsue, T. and Uchida, I., Electrochemical preparation of ultrathin polypyrrole film at microarray electrodes. *J. Phys. Chem*., 1991, **95**, 9042–9044; Sayre, C. N. and Collard, D. M., Deposition polyaniline on microcontact printed self-assembled monolayer of ω-functionalised alkanethiols. *J. Mater. Chem*., 1997, **7**, 909–912; Sayre, C. N. and Collard, D. M., Micron scale patterning of conjugated polymers on microcontact printed patterns of self-assembled monolayers. *Synth. Met*., 1997, **84**, 322–329.
29. Seshadri, K., Atre, S. V., Tao, Y-T., Lee, M. T. and Allara, D. L., Synthesis of crystalline, nanometer scale, $-(CH_2)_x-$ clusters and films on gold surfaces. *J. Am. Chem. Soc*., 1997, **119**, 4698–4711.
30. Tao, Y-T., Pandian, K. and Lee, W. C., Microfabrication of interdigitated polyaniline/polymethylene patterns on a gold surface. *Langmuir*, 1998, **14**, 6158–6166; Nirmala Grace, A. and Pandian, K., Polypyrrole polymethylene pattern on Au using microcontact printing (μ-CP) technique. *J. Solid State Electrochem*., 2003, **7**, 296–300.
31. Sayre, C. N. and Collard, D. M., Electrooxidative polymerization pf polypyrrole and polyaniline on self-assembled monolayer modified electrodes. *Langmuir*, 1997, **13**, 714–722.

Received 24 February 2003; revised accepted 3 May 2003

On the origin of non-uniform surface electrochemical potentials on the Delhi iron pillar

R. Balasubramaniam
Department of Materials and Metallurgical Engineering,
Indian Institute of Technology Kanpur, Kanpur 208 016, India

The origin of non-uniform surface electrochemical potentials on the Delhi iron pillar has been addressed based on modern electrochemical theory of passivation. Surface potentials have been related to the differences in thickness and nature of the protective passive film on the exposed surface of the pillar. The most protective passive scale is present in the upper region of the pillar.

THE corrosion-resistant Delhi iron pillar has been attracting the attention of archaeologists, scientists, engineers and scholars for well over two centuries, eager to unravel the many hidden mysteries of the pillar[1]. Several new insights on the Delhi iron pillar have been obtained recently[2]. The excellent atmospheric corrosion resistance of the pillar has been attributed to the formation of a protective passive film on the surface. The nature of this protective passive film has been elucidated[3] by analysing the undisturbed rust of the pillar utilizing modern characterization methods[4]. The process of protective film-formation under atmospheric exposure conditions has also been explained[3]. The protective passive film mechanism of corrosion resistance of the Delhi iron pillar has been recently questioned in the press, wherein it was quoted that surface electrochemical potentials measured on the pillar revealed differences[5]. The direct relevance of surface electrochemical potentials (measured in aqueous solutions) to atmospheric corrosion is not evident because alternate wetting and drying cycles are involved in atmospheric corrosion. Moreover, it is now well established that the nature and rates of electrochemical (anodic and cathodic) reactions that occur during atmospheric corrosion vary significantly during the course of *each* wetting and drying cycle[6]. Nevertheless, the development of non-uniform surface electrochemical potentials on the Delhi iron pillar does not negate the protective passive film mechanism of corrosion resistance of the pillar. The present communication will explore the origin of non-uniform surface electrochemical potentials utilizing modern electrochemical theory of passivation.

Passivity of metals has been a subject of significant research. The nature of the passive films that form on a wide variety of materials has been explored utilizing special electrochemical characterization techniques like impedance spectroscopy[7]. The mechanism of passive film-formation can be understood by modern electrochemical theory, with the aid of polarization diagrams. The polarization diagram is a plot between the potential (i.e. the thermodynamic axis) and current density (i.e. the kinetic axis). The changes in the current density as a function of polarization (i.e. deviation of potentials away from equilibrium) are represented in these polarization diagrams, and several processes related to corrosion (and electrochemistry) can be easily understood utilizing these diagrams. The anodic polarization diagram for a metal exhibiting passivity (i.e. condition of corrosion resistance due to formation of an adherent non-dissolving passive film on anodic polarization under oxidizing conditions) is schematically depicted in Figure 1. It must be remembered that experiments have to be performed by controlling the potential and measuring the current (i.e. either potentiostatically or potentiodynamically) rather than vice versa, in order to understand the passivation phenomenon[8]. In the discussion below, it is emphasized that a freshly prepared (and not oxide or surface-film covered) surface is exposed to the aqueous environment and the anodic polarization is begun immediately on immersion. At the equilibrium reversible potential of the metal (E_{rev}), the ex-

e-mail: bala@iitk.ac.in

change current density (i_o) depicts the rate of the forward reaction (i.e. corrosion) being equal to the rate of the reverse reaction (i.e. reduction). On anodically polarizing the material, thermodynamic conditions for the formation of a stable surface film are established at point A (Figure 1). Surface film is meant here in the general sense, without specifying the exact nature of the film. This is because the nature of the surface film that results in passivity could be the corrosion product layer, oxide/oxyhydroxide film, adsorbed oxygen or adsorbed ions[7–9]. Different mechanisms operate in different alloy systems[9]. On further anodically polarizing the material, the passive film nucleates on the surface from point B onwards and this indicates the potential for initiation of passivity (E_{ip}). The location of the points A and B with respect to E_{rev} depends upon the alloy system[10–16]. On further increasing the potential, the film starts covering the surface laterally and at optimum coverage, the critical current density (i_{crit}) is achieved (point C), corresponding to which the primary passivation potential (E_{pp}) is defined. On further anodic polarization beyond E_{pp}, the surface passive film completely covers the surface and the current density decreases with increasing anodic polarization until the point D, when the passive film completely covers the surface. The potential corresponding to point D is referred to as the potential for complete passivation (E_{cp}). On polarizing past this potential, the current density remains constant with increasing potential in the passive range (Figure 1). This is the region that has to be viewed carefully in order to understand the non-uniform surface electrochemical potentials obtained on the Delhi iron pillar. On further anodically polarizing the material, several reactions can lead to the destruction of passivity (i.e. indicated by increasing current density with increasing potential). Some of these processes are oxygen evolution, transpassive dissolution due to conversion of the passive film-forming ion to a higher oxidation state, pitting caused by destabilization of the passive film due to the presence of halide ions or changes in the nature of the passive film (for example anodizing, wherein there is a change in porosity of the passive film).

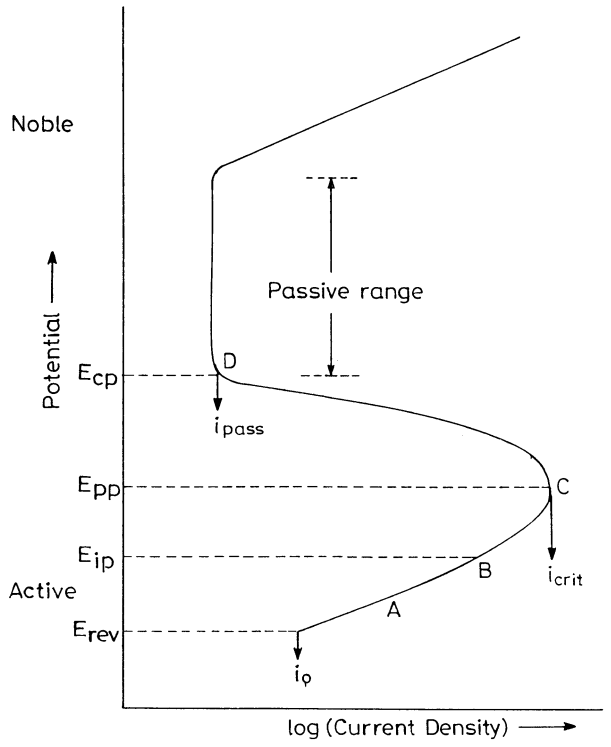

Figure 1. Schematic anodic polarization diagram for an active–passive metal illustrating important passivity parameters. It is assumed that the surface of the metal was freshly prepared and the anodic polarization begun immediately on immersion.

In the passive region, the current density remains constant with increasing anodic polarization, which is due to thickening of the passive film[17]. It is important to note the fine dimensions of the passive film[9]. The current density remains constant over a significant range of potential in the passive range, and this is called the passive current density (i_{pass}). The passive current density is dictated by the constant rate of dissolution of the metal ions into the electrolyte from the passive film surface. Thickening of the film accommodates the increasing anodic positive potentials in the passive range. In case the potential is held constant in the passive range after the formation of the passive film, the current density decreases with time[17]. This has generally been modelled by logarithmic growth kinetics[9,17]. Therefore, the time factor is also an important consideration while discussing passivation. An example of the same is shown in Figure 2 for Dhar iron pillar. The potentiodynamic polarization curve for iron in a borate-buffered solution of pH 8.4 is presented in Figure 2 *a*. The borate-buffered solution was chosen because the pH of rust is alkaline. In a separate experiment, the sample was polarized beyond the critical current density to a potential of + 250 mV vs SCE in the passive region and the current density was followed as a function of time at this fixed potential (Figure 2 *b*). The decreasing current density with time indicates growth of passive film on the surface, and the passive film growth kinetics can be modelled utilizing such data.

The development of free corrosion potentials needs to be addressed. Modern electrochemical theory states that equilibrium corrosion condition is obtained when the net cathodic rate is equal to the net anodic rate. Practically, this implies that the free corrosion potential will be established at the potential where the cathodic polarization curve (i.e. of the cathodic reaction) intersects the anodic polarization curve. The rate of the anodic reaction is therefore directly related to the rate of chemical reduction reaction(s) at cathodic areas. The cathodic reaction in deaerated solutions is hydrogen-evolution, given by

$$2H^+ + 2e \rightarrow H_2 \quad \text{(acidic)} \qquad (1)$$

$$2H_2O + 2e \rightarrow H_2 + 2OH^- \quad \text{(neutral or alkaline)} \qquad (2)$$

The hydrogen-evolution reaction proceeds rapidly in acids, but slowly in alkaline or neutral media. The corrosion rate of ancient Indian irons in aqueous conditions, especially when a protective passive film does not cover the surface, is much higher than mild steel of similar composition because of the presence of entrapped slag inclusions[18–20]. Dissolved oxygen in the electrolyte takes part in the cathodic reaction in accordance with one of the following reactions:

$$4H^+ + O_2 + 4e \rightarrow 2H_2O \quad \text{(acidic)} \tag{3}$$

$$O_2 + 2H^+ + 4e \rightarrow 2OH^- \quad \text{(neutral/alkaline)} \tag{4}$$

$$2H_2O + O_2 + 4e \rightarrow 4OH^- \quad \text{(alkaline)} \tag{5}$$

Dissolved oxygen reacts with hydrogen/water adsorbed at random on the iron surface, independent of the presence or absence of impurities in the metal. Therefore, the oxidation reaction proceeds as rapidly as oxygen reaches the metal surface.

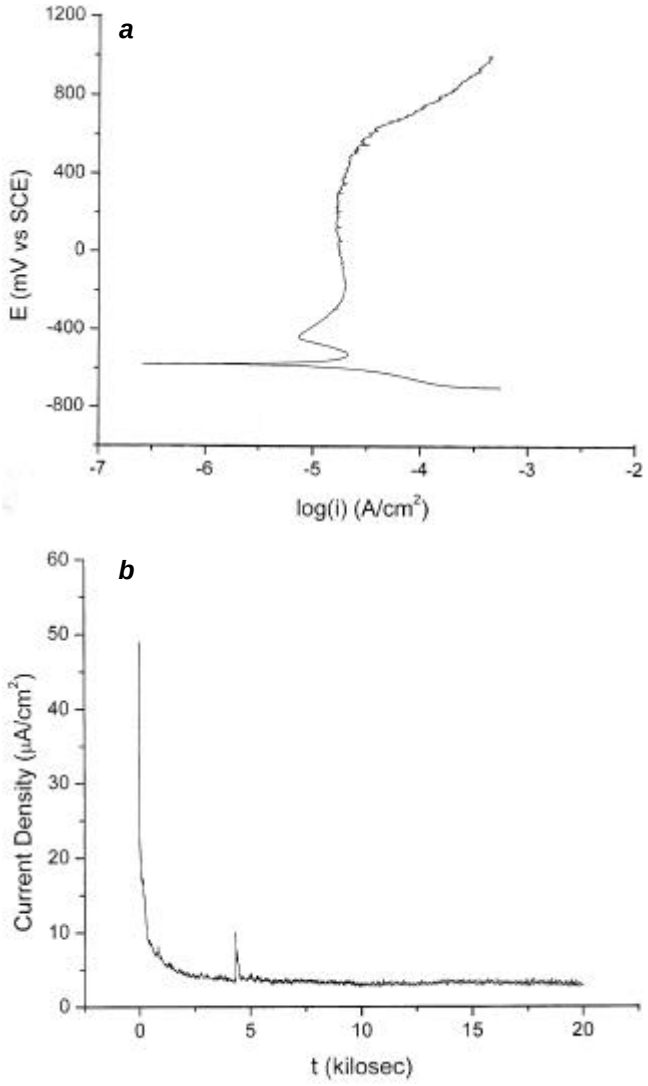

Figure 2. Dhar iron pillar sample. ***a***, Potentiodynamic polarization curve in a borate-buffered solution, pH 8.4; and ***b***, Variation of passive current density with time after the sample was polarized to and maintained at a potential of + 250 mV vs SCE in the passive range.

The corrosion or rusting of iron in the atmosphere occurs by the well-known reaction[6]

$$2Fe + H_2O + {}^1/_2\, O_2 \rightarrow 2FeOOH \tag{6}$$

The atmospheric corrosion process is electrochemical in nature. The above reaction can be conveniently considered as partial oxidation (anodic) and reduction (cathodic) reactions. Metal dissolution is the anodic partial reaction. The dominant cathodic reaction is, of course, the reduction of oxygen, eq. (4), while the hydrogen reduction, eq. (1), may also occur. As the electrolyte on the surface of iron-based materials is well buffered in the neutral and alkaline range under atmospheric corrosion condition, the rate of hydrogen reduction is generally much lower than the rate of oxygen reduction. A third type of cathodic reaction, provided below, must also be considered in the atmospheric corrosion of iron[6,21]:

$$8FeOOH + Fe^{2+} + 2e \rightarrow 3Fe_3O_4 + 4H_2O \tag{7}$$

The above reduction reaction becomes important during atmospheric wetting-and-drying cycles, when the oxygen reduction rate is limited by the presence of a thick electrolyte layer on the surface.

The oxygen reduction reaction will be considered to illustrate the development of free corrosion potential (FCP) or mixed potential under atmospheric corrosion conditions. The cathodic polarization curve corresponding to oxygen reduction reaction can intersect the anodic polarization curve at different locations and, based on this, different conditions of passivity (stable or unstable) or active behaviour can be realized[8,22]. Three possible situations are depicted in Figure 3. In Figure 3 *a*, the cathodic polarization curve intersects the anodic curve in the active region and the FCP is established at the potential corresponding to the intersection of both these curves. The metal corrodes in the active state. In practical cases, this situation generally depicts corrosion of fresh surface of iron, free from any surface film. The experimental polarization diagram presented in Figure 2 *a* represents this condition, because the potentiodynamic polarization scan was begun immediately after immersion of the polished sample. In case the anodic polarization curve intersects the cathodic polarization curve *only* in the passive region, then the FCP would be established in the passive region. This is the condition of stable passivity (Figure 3 *b*). When the cathodic polarization curve intersects the anodic polarization curve as shown in Figure 3 *c*, there are three potentials at which the anodic and cathodic current densities are equal. The FCP that the material will achieve depends on its prior surface condition. In case a fresh surface is exposed without any film present, then the FCP would establish in the active region, whereas if there were a pre-existing passive film, the FCP would establish in the passive region. The schematic depicted in Figure 3 *c* is

indicative of unstable passivity and the experimental polarization diagram for this situation would show the existence of a cathodic loop[8]. The above discussion establishes that surface electrochemical potential depends upon the nature of the surfaces as well as the cathodic reaction kinetics.

In order to understand the electrochemical behaviour of Delhi iron pillar surfaces, it would have been ideal to experiment on samples obtained from the pillar. However, as such samples are not available, electrochemical polarization studies were conducted on a corrosion-resistant Gupta-period iron. The iron was obtained in the form of a clamp from the Deogarh temple, which has been conservatively dated to about AD 600 (ref. 23). A portion of the iron clamp was sectioned with a diamond blade. Anodic polarization curves were obtained for the iron surface under two different conditions. The adherent rust scale was removed from two sample surfaces, while retaining the scale on two other surfaces. The potentiodynamic polarization experiments were conducted in freely aerated double-distilled water containing 0.001 M Na_2SO_4. Double-distilled water simulates moisture condensation during atmospheric exposure and the small amount of salt aids electrolytic conductivity. The experimental results are presented in Figure 4. The FCP was established in the passive region for both the samples that had their surface scales intact, whereas the two samples without surface scale exhibited active corrosion. It is also important to note that the passive ranges in the case of the rust-covered samples were quite large. Minor differences in the nature of the passive film at the two different locations can also be discerned in the potentiodynamic polarization curves of the rust-covered samples (Figure 4). In an analogous manner, surface electrochemical potentials are expected to be different at different locations on the Delhi iron pillar, depending upon the nature of the surface. As shown in this study on an iron sample taken from a Gupta-period temple, the surface electrochemical potential of a rust-covered surface would be nobler compared to rust-free surfaces.

The development of non-uniform surface electrochemical potential on protective passive-scale-covered surface of the Delhi iron pillar must have its origins in the differing thickness of the protective passive film. The most protective film will exhibit a large passive range and noble FCP. In addition to the differing thickness, the nature of the protective passive film at different locations is also important, because differences in its nature would also manifest as differences in measured FCPs and anodic electrochemical polarization behaviour. The results of the surface electrochemical potential study on the Delhi iron pillar are not available. However, the nature of surface

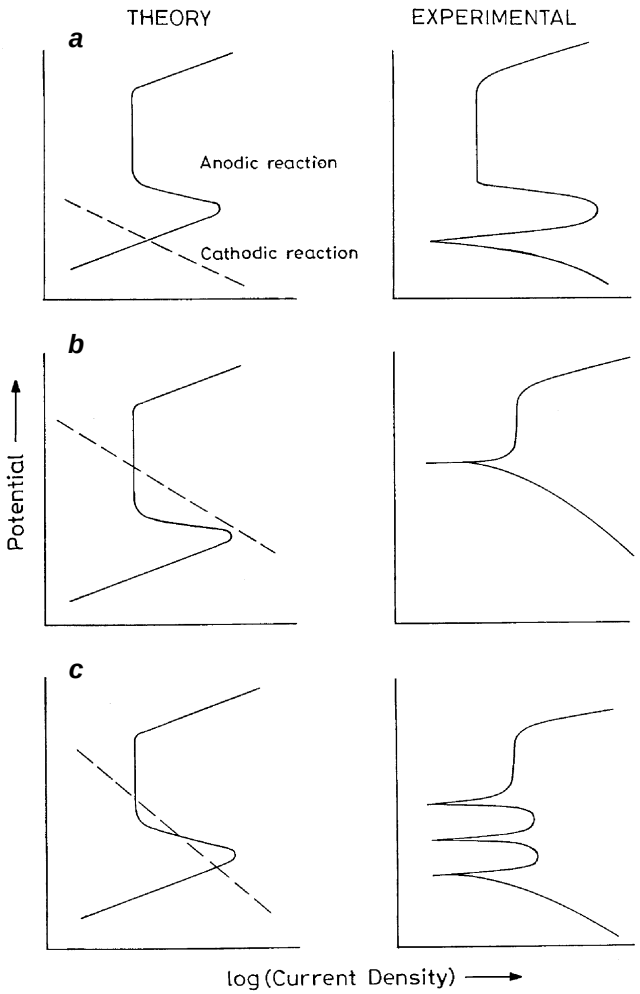

Figure 3. Schematic illustration outlining the theoretical aspects governing the development of experimental polarization diagrams. ***a***, Active behaviour; ***b***, Stable and ***c***, Unstable passive behaviour.

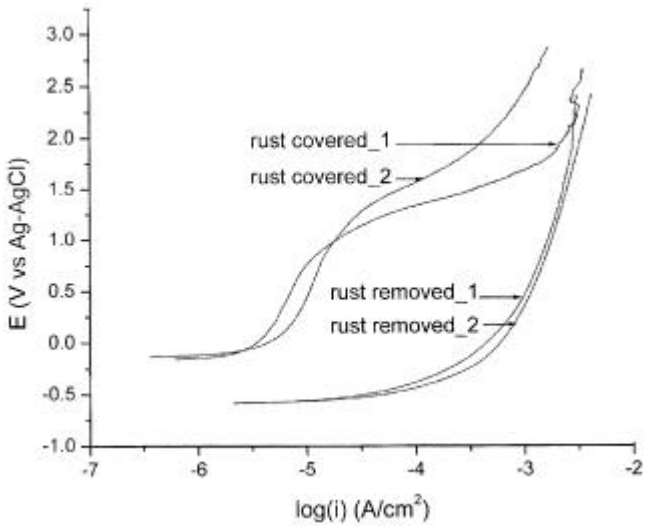

Figure 4. Potentiodynamic polarization results for Gupta-period iron conducted in freely aerated double-distilled water containing 0.001 M Na_2SO_4. Results have been presented for two samples with an adherent rust layer present on the surface and for two other samples without adherent rust.

potentials can be predicted based on modern electrochemical theory and the available knowledge of the surface of the pillar[2]. The most noble potentials will be obtained in the upper regions of the pillar because this is the location where the rust has been disturbed the least. Complementarily, the measured passive ranges will be quite large. On the other hand, the surface potentials measured in the lower region of the pillar will be more active compared to the potentials measured higher up in the pillar. Lower passive ranges are also anticipated in the lower regions of the pillar. Human-contact activities are the main cause of differing nature of surface-protective passive film. The lower regions of the pillar were in contact with humans before the Archaeological Survey of India constructed an iron grill cage in 1997, in order to prevent people from damaging the pillar (see cover page of *Current Science* 25 December 1997). In fact, the pillar used to be swarmed with people trying to clasp their hands around it, with their backs on the pillar, in the belief that accomplishment of such a task would bestow luck. The protective passive film is, therefore, much thinner on the pillar surface till about 8 ft from the ground level, due to the constant polishing action by the visiting public. The recent greasing of the pillar at several locations and its subsequent removal, after reports of the same appeared in the press[24], would also have additionally resulted in changes in the thickness and nature of the protective film. In contrast to the locations in the bottom regions, the nature of the protective passive film is relatively undisturbed in the upper regions of the Delhi iron pillar. This was precisely the reason for choosing rust samples from these locations for characterization purposes[4].

In summary, the development of non-uniform surface electrochemical potential on the Delhi iron pillar has been addressed. This has been related to the differences in thickness and nature of the protective passive film on the exposed surface of the pillar. The most protective passive scale is present in the upper region of the pillar.

1. Anantharaman, T. R., *The Rustless Wonder – A Study of the Delhi Iron Pillar*, Vigyan Prasar, New Delhi, 1996.
2. Balasubramaniam, R., *Delhi Iron Pillar: New Insights*, Indian Institute of Advanced Study, Shimla and Aryan Books International, New Delhi, 2002.
3. Balasubramaniam, R., On the corrosion resistance of the Delhi iron pillar. *Corros. Sci*., 2000, **42**, 2103.
4. Balasubramaniam, R. and Ramesh Kumar, A. V., Characterization of Delhi iron pillar rust by X-ray diffraction, Fourier infrared spectroscopy and Mössbauer spectroscopy. *Corros. Sci*., 2000, **42**, 2085.
5. Iron Pillar and Nano Powder. *The Hindu*, Science and Technology Section, 29 August 2002.
6. Stratmann, M., The atmospheric corrosion of iron – A discussion of the physico-chemical fundamentals of this omnipresent corrosion process. *Ber. Bunsenges. Phys. Chem*., 1990, **94**, 626.
7. Frankenthal, R. P. and Kruger, J. (eds), *Passivity of Metals*. The Electrochemical Society Corrosion Monograph Series, Princeton, USA, 1978.
8. Jones, D. A., *Principles and Prevention of Corrosion*, Maxwell Macmillan International Publishing Group, New York, 1992, pp. 115–141.
9. MacDougall, B. and Graham, M. J., Growth and stability of passive films. in *Corrosion Mechanisms in Theory and Practice* (ed. Marcus, P.), Marcel Dekker, New York, 2002, pp. 189–216.
10. Stern, M. and Wissenberg, H., The influence of noble metal alloy additions on the electrochemical and corrosion behaviour of titanium. *J. Electrochem. Soc*., 1959, **106**, 759.
11. Osozawa, K. and Engell, H. -J., The anodic polarization curves of iron–nickel–chromium alloys. *Corros. Sci*., 1966, **6**, 389.
12. Griess, J. C., Crevice corrosion of titanium in aqueous salt solutions. *Corrosion*, 1968, **24**, 96.
13. Goetz, R., Laurent, J. and Landolt, D., The influence of minor alloying elements on the passivation behaviour of iron–chromium alloys in HCl. *Corros. Sci*., 1985, **25**, 1115.
14. Schutz, R. W. and Thomas, D. E., *Metals Handbook*, ASM International, Metals Park, USA, 1987, vol. 13, 9th edn, p. 669.
15. Kirchheim, R. and Heine, B., Korrosionsgeschwindigkeiten von eisen, chrom und eisen–chrom–leizierungen im passivzustand. *Z. Metallk.*, 1990, **81**, 726.
16. Zhu, X. M. and Zhang, Y. S., Investigation of the electrochemical corrosion behavior and passive film for Fe–Mn, Fe–Mn–Al and Fe–Mn–Al–Cr alloys in aqueous solutions. *Corrosion*, 1998, **54**, 3.
17. Stern, M., Evidence for a logarithmic oxidation process for stainless steel in aqueous systems. *J. Electrochem. Soc*., 1959, **106**, 376.
18. Ramesh Kumar, A. V. and Balasubramaniam, R., Corrosion product analysis of ancient corrosion resistant Indian iron. *Corros. Sci*., 1998, **40**, 1169.
19. Balasubramaniam, R., A new study of the Dhar iron pillar. *Indian J. History Sci*., 2002, **37**, 115.
20. Puri, V., Balasubramaniam, R. and Ramesh Kumar, A. V., Corrosion behaviour of ancient 1500-year old Gupta iron. *Bull. of Metals Mus.*, 1997, **28**, 1.
21. Evans, U. R. and Taylor, C. A. J., Mechanism of atmospheric rusting. *Corros. Sci*., 1972, **12**, 227.
22. Chatterjee, U. K., Bose, S. K. and Roy, S. K., *Environmental Degradation of Metals*, Marcel Dekker, New York, 2001, pp. 34–36.
23. Vats, M. S., The Gupta temple at Deogarh. *Mem. Archaeol. Surv. India*, No. 70, 1952.
24. When science leaves its stain on history. *Times of India*, 19 March 2001.

ACKNOWLEDGEMENT. I would like to acknowledge the co-operation and assistance of the Archaeological Survey of India.

Received 5 February 2003; revised accepted 7 May 2003